Time domain-based oscillatory feature extraction for high spatiotemporal resolution neurophysiologic data

Liang Ma
Department of Biomedical Engineering
Columbia University
New York, USA
lm3397@columbia.edu

Tristan Sands
Department of Neurology
Columbia University Irving Medical Center
New York, USA
tts27@cumc.columbia.edu

Dion Khodagholy
Department of Electrical Engineering
University of California Irvine
Irvine, USA
dion.kh@uci.edu

Jennifer Gelinas
Department of Pediatrics
University of California Irvine
Irvine, USA
gelinasj@hs.uci.edu

***Abstract*— Organic electronics can be leveraged to create conformable, biocompatible, high density sensing arrays that generate high spatiotemporal resolution neurophysiologic data from novel experimental paradigms. A main priority for analysis of this data is detection of oscillations, due to their association with information processing and effective use as targets for network-based closed-loop therapeutics. However, current frequency-based approaches are hindered by the non-stationary, irregular waveforms that comprise neural oscillations, and require bulky, rigid, high power consuming hardware for implementation. Here, we developed a low latency, time domain-based method that detects and characterizes oscillations without the need for *a priori* knowledge of signal characteristics. We tested this approach using data generated by arrays of organic electronic electrodes implanted in developing mice harboring a gene mutation that results in developmental disability and were able to identify key signal motifs. This work opens avenues for advanced, closed-loop analytics applicable to neurologic disorders.**

Keywords—neurophysiology, oscillation, organic electronics

I. Introduction

Diagnosis and monitoring of treatment response for a variety of neurologic disorders requires interpretation of brain-derived neurophysiologic data. This data is comprised of a complex mixture of periodic and aperiodic components. The periodic components take the form of transient oscillations, which reflect ongoing information processing and are dysregulated in many neurologic disorders[1]. Currently, interpretation relies heavily on expert visual identification of oscillations based on various signal features in the raw time series (voltage/time) data[2]. High heterogeneity of signals between patients and across disease states, the co-existence of oscillations with broad-band transients, and lack of ideal sinusoidal kernel have limited the efficacy of frequency-based computational approaches for clinical purposes[3]. Implementation of any automated detection of these oscillations also requires *a priori* knowledge of key features which are often unknown in disease states, and necessitates bulky hardware that poses challenges for incorporation into implantable closed-loop devices[4]. Yet, as the sensitivity and density of neural interface devices increase, visual pattern identification by human experts becomes impractical. Organic electronic neural interface devices have been shown permit simultaneous acquisition of hundreds of channels at 20 kHz sampling rate from a variety of experimental paradigms, ranging from human cortex to mouse models of pediatric epilepsy[5], [6]. This study presents a time domain-based oscillatory feature extraction algorithm that can be effectively applied to such varied, high spatiotemporal resolution datasets and implemented with low latency and minimal hardware requirements. We use this algorithm on a novel dataset recorded from immature mice expressing a KCNQ3 mutation that results in developmental disability[7] and demonstrate its capacity to provide an unbiased readout of oscillatory features.

II. Devices and Neural Data

A. Organic electronics generate high spatiotemporal resolution neurophysiologic data

Organic electronics possess properties that are beneficial for design of neural interface devices, including conformability, efficient abiotic/biotic interface, biocompatibility, and capacity to form scalable, miniaturizable, high density electrode arrays[8]. Devices with conducting polymer-based electrodes can be nanofabricated into form factors amenable to surface or depth recording from the brain. Furthermore, they can be customized to acquire neurophysiologic signals from preparations typically inaccessible to this monitoring, such as the fragile tissue of the developing brain *in vivo* (Figure 1A). These devices support sampling of signals at 20 kHz across hundreds of individual channels, generating high spatiotemporal resolution datasets (Figure 1B, upper). Signals are highly non-stationary, with complex waveforms and spectral features, as exemplified in the data acquired from a mouse pup 13 days after birth (PND 13; Figure 1B, lower).

III. Time Domain Method

A. Time domain-based oscillatory feature extraction

To extract information regarding the presence of oscillations in such data in the time domain, the raw LFP is first z-scored to normalize the amplitude values. A peak detection algorithm was then applied, wherein local maxima were simply identified as data samples with values larger than neighboring data samples. Minimum peak height was specified using a threshold based on a fraction of the wideband noise floor, which was customized based on signal to noise ratio of the data. Minimum peak width was determined by sampling rate of the data and practically guided by physiologic limits of oscillations within *in vivo* neural networks (maximum of several hundred Hz; Figure 2A). Detected peaks were characterized by their width at half maximum and peak height (Figure 2B). From

2024 IEEE International Electron Devices Meeting (IEDM) | 979-8-3503-6542-9/24/$31.00 ©2024 IEEE | DOI: 10.1109/IEDM50854.2024.10873387

XXX-X-XXXX-XXXX-X/XX/$XX.00 ©20XX IEEE

Authorized licensed use limited to: Access paid by The UC Irvine Libraries. Downloaded on April 30,2025 at 01:20:51 UTC from IEEE Xplore. Restrictions apply.

these data, oscillatory period for each peak was calculated, allowing for visualization of the distribution of individual periods across the data (Figure 2C). Next, peaks were grouped into putative discrete oscillations based on the similarity of their oscillatory period after discarding any peaks within the oscillatory period (i.e. a nested oscillation). Neighboring peaks with oscillatory periods that differed by less than 5% were considered members of an oscillation, with a gap of greater than the oscillatory period signifying the end of this oscillation. These putative oscillations could then be characterized by an array of features, such as mean amplitude, duration, number of oscillatory cycles and root mean square power. Our time domain-based approach was compared with a conventional wavelet transform (a frequency-based approach), using sample data with known characteristics to allow evaluation of results relative to a gold standard. Sample data was extracted from hippocampal recordings during rapid eye movement (REM) sleep, an epoch characterized by prominent theta oscillations (5-8 Hz) with nested gamma oscillations (30-100 Hz; Figure 3A). The distribution of oscillatory periods detected by the time domain approach was bimodal, consistent with detection of both types of oscillations (Figure 3B, left). In contrast, the wavelet transform detected only the theta peak (Figure 3B, right). Thus, the time domain approach is more sensitive to the higher frequency oscillations without requiring multiple data pre-processing steps.

B. Time domain-based analysis of novel neurophysiologic dataset

Mouse models of pediatric neurologic disease are critical to understand how dysregulation of neural networks emerges. The R231H mutation in *Kcnq3* is orthologous to the human mutation which is associated with developmental disability and epileptiform discharges in children. We implanted wild-type and mutant mouse pups with conducting polymer-based electrode arrays to acquire high spatiotemporal resolution data from cortex. Raw LFP traces revealed stark differences in oscillatory features between wildtype and mutant mice, but without *a priori* knowledge of how oscillations are dysregulated by the KCNQ3 mutation, characterization was challenging (Figure 4A). To quantitatively compare these datasets, the time domain-based oscillatory detection approach was employed, followed by characterization of oscillatory features. Using principal components analysis for dimensionality reduction, data derived from wildtype and mutant mice was demonstrated to be separable (Figure 4B), enabling further analysis of physiologic and pathologic oscillations.

IV. Discussion

Implementation of this time domain-based, unbiased oscillatory extraction algorithm paves the way for systematic analysis of novel datasets generated by high spatiotemporal resolution neural interface devices. The peak-by-peak approach employed allows accurate identification of true oscillations, as defined by rhythmic activity with a narrow, consistent oscillatory period. These oscillations are most likely to have defined roles within physiologic networks and characteristic dysfunction in disease states, making them key targets for detection and implementation of closed-loop therapeutics[9], [10], [11]. This methodology is also robust to the perpetually evolving bursts of oscillatory cycles characteristic of neural activity, and their irregular (non-sinusoidal) waveforms that typically present challenges for frequency-based approaches. Such features are exemplified in neurophysiologic signals of the developing brain, and the time domain-based algorithm efficiently parsed oscillatory motifs from this data. Furthermore, it can be implemented with simple arithmetic, resulting in capacity for low-latency processing with minimal hardware requirements. Thus, implementation could potentially be accomplished using conformable, organic electronic transistors, setting the stage for fully implantable, conformable, and biocompatible neural processing devices[12], [13], [14].

Acknowledgment

This work was supported by University of California Irvine and Columbia University Irving Medical Center. The device fabrication was performed at Columbia Nano-Initiative.

References

[1] T. Donoghue *et al.*, "Parameterizing neural power spectra into periodic and aperiodic components," *Nat Neurosci*, vol. 23, no. 12, pp. 1655–1665.

[2] M. A. Kural *et al.*, "Criteria for defining interictal epileptiform discharges in EEG: A clinical validation study," *Neurology*, vol. 94, no. 20, pp. E2139–E2147, May 2020.

[3] C. S. Herrmann, S. Rach, J. Vosskuhl, and D. Strüber, "Time-frequency analysis of event-related potentials: a brief tutorial," *Brain Topogr*, vol. 27, no. 4, pp. 438–450, 2014

[4] K. W. Scangos *et al.*, "Closed-loop neuromodulation in an individual with treatment-resistant depression," *Nat Med*, vol. 27, no. 10, 2021.

[5] A. R. Hassan *et al.*, "Translational Organic Neural Interface Devices at Single Neuron Resolution," *Adv Sci (Weinh)*, vol. 9, no. 27, Sep. 2022,.

[6] A. N. Shore *et al.*, "Reduced GABAergic Neuron Excitability, Altered Synaptic Connectivity, and Seizures in a KCNT1 Gain-of-Function Mouse Model of Childhood Epilepsy," *Cell Rep*, vol. 33, no. 4, Oct. 2020.

[7] T. T. Sands *et al.*, "Autism and Developmental Disability Caused by KCNQ3 Gain-of-Function Variants," 2019.

[8] D. Khodagholy *et al.*, "NeuroGrid: recording action potentials from the surface of the brain," *Nat Neurosci*, vol. 18, no. 2, pp. 310–315, Feb. 2015.

[9] D. Khodagholy, J. N. Gelinas, and G. Buzsáki, "Learning-enhanced coupling between ripple oscillations in association cortices and hippocampus," *Science*, vol. 358, no. 6361, pp. 369–372, Oct. 2017.

[10] Z. Zhao, C. Cea, J. N. Gelinas, and D. Khodagholy, "Responsive manipulation of neural circuit pathology by fully implantable, front-end multiplexed embedded neuroelectronics," *Proc Natl Acad Sci U S A*, vol. 118, no. 20, 2021.

[11] J. N. Gelinas, D. Khodagholy, T. Thesen, O. Devinsky, and G. Buzsáki, "Interictal epileptiform discharges induce hippocampal-cortical coupling in temporal lobe epilepsy," *Nat Med*, vol. 22, no. 6, pp. 641–648, Jun. 2016.

[12] Z. Zhao, G. D. Spyropoulos, C. Cea, J. N. Gelinas, and D. Khodagholy, "Ionic communication for implantable bioelectronics," *Sci Adv*, vol. 8, no. 14, p. 7851, Apr. 2022.

[13] C. Cea, G. D. Spyropoulos, P. Jastrzebska-Perfect, J. J. Ferrero, J. N. Gelinas, and D. Khodagholy, "Enhancement-mode ion-based transistor as a comprehensive interface and real-time processing unit for in vivo electrophysiology," *Nat Mater*, vol. 19, no. 6, pp. 679–686, Jun. 2020.

[14] P. Jastrzebska-Perfect *et al.*, "Mixed-conducting particulate composites for soft electronics," *Sci Adv*, vol. 6, no. 17, 2020.

Authorized licensed use limited to: Access paid by The UC Irvine Libraries. Downloaded on April 30,2025 at 01:20:51 UTC from IEEE Xplore. Restrictions apply.

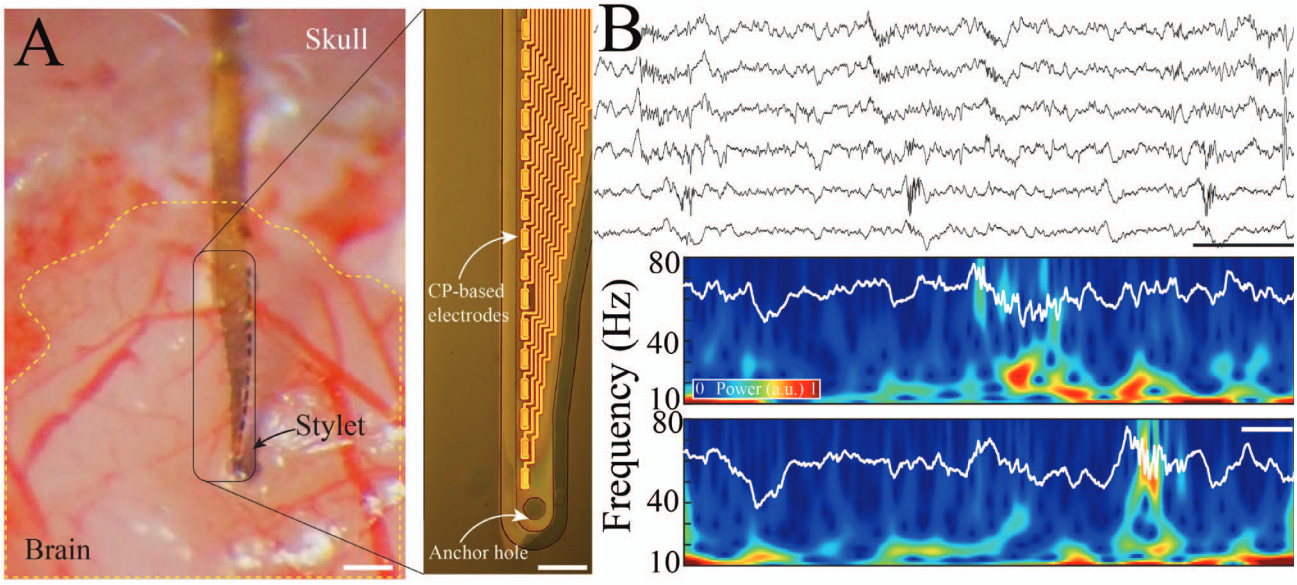

Fig. 1: Conformable organic electronics acquire high spatiotemporal resolution neurophysiologic data. A) Photomicrography of linear array of conducting polymer-based electrodes in a conformable parylene C substrate prior to insertion into the brain of a mouse pup (left; scale bar 100 µm) and zoomed in view demonstrating device architecture (right; scale bar 50 µm). B) Sample raw local field potential traces obtained from 5 conducting polymer-based electrodes implanted in a PND 13 mouse pup (upper; scale bar 1 s, 500 µV) and two sample spectrograms derived from raw data using a wavelet transform (lower; scale bar 200 ms).

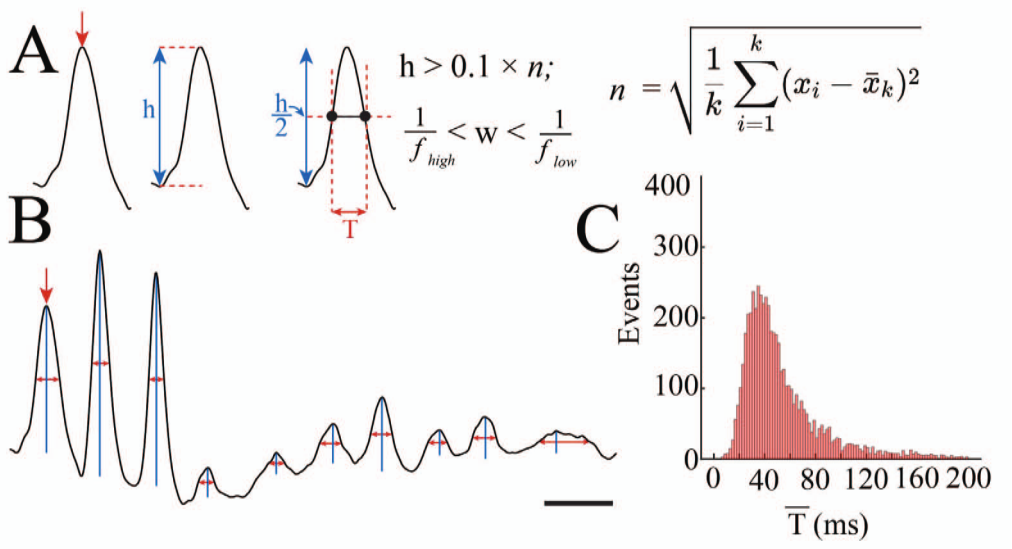

Fig 2: Time domain-based approach to oscillatory detection. A) Peaks are identified by local maxima (red arrow), followed by extraction of peak height (h; blue arrow) and peak width at half maximum height (T; red arrow). Minimum peak height is determined based on noise (n) floor derived from the signal (x) standard deviation. Minimum peak width is determined based on sampling rate and physiological bandwidth (f_{low} - f_{high}). B) Sample raw LFP trace with oscillatory peak detection (scale bar 100 ms). C) Histogram of detected peak widths in a sample dataset.

Authorized licensed use limited to: Access paid by The UC Irvine Libraries. Downloaded on April 30,2025 at 01:20:51 UTC from IEEE Xplore. Restrictions apply.

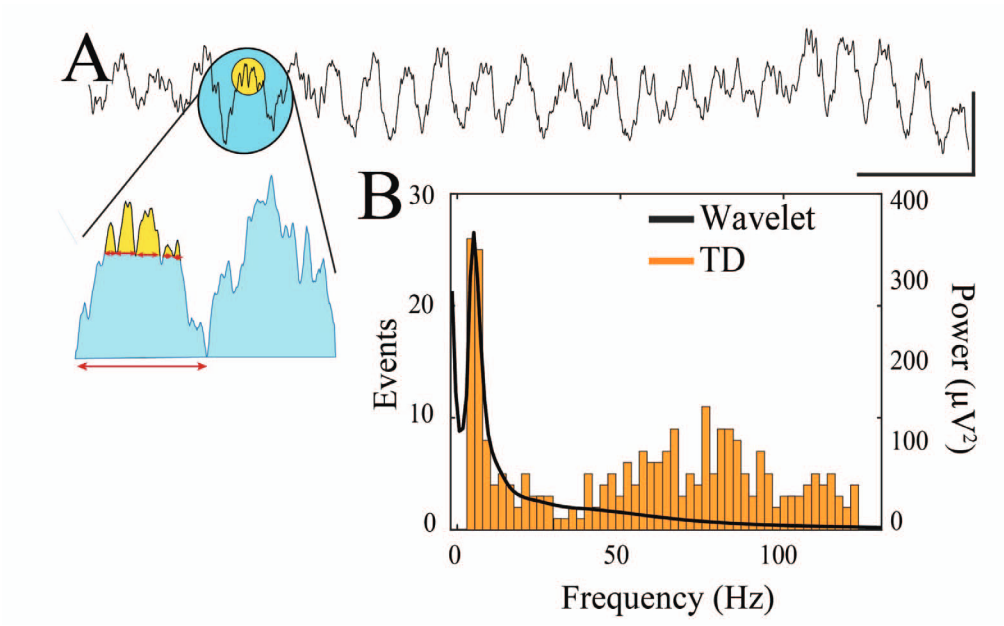

Fig 3. Time-domain oscillatory detection of nested high frequencies. A) Sample traces of a REM epoch with highlighted theta oscillation (blue) and nested gamma oscillations (yellow) with their corresponding peak dectetion. B) Histogram of frequency content of the REM epoch derived using time-domain detection (orange) showing bimodality with prominent theta and gamma oscillatory activity without the need for additional pre-processing. Black trace shows the analytic wavelet transform of the same trace with a notable theta peak but absent gamma peak.

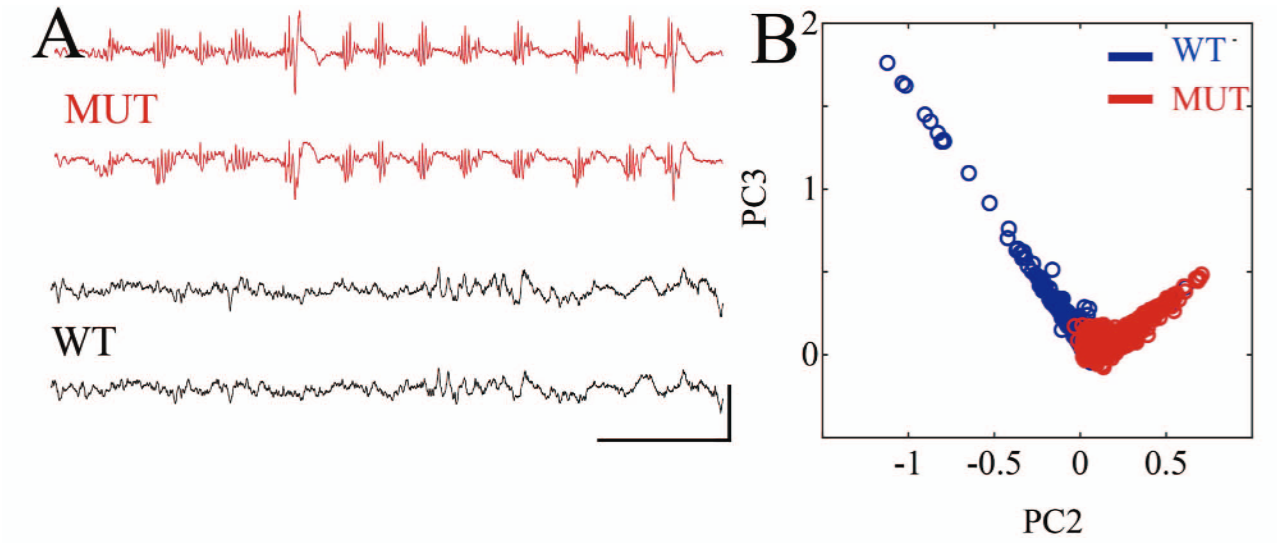

Fig. 4: Oscillatory activity patterns in wildtype and mutant immature mice. A) Sample raw LFP traces from KCNQ3 mutant (MUT) mice (red) and wildtype (WT) mice (black) at PND 13. B) Principal component analysis of oscillatory features extracted from time domain approach effectively differentiates signals acquired from wildtype and mutant mice.

Authorized licensed use limited to: Access paid by The UC Irvine Libraries. Downloaded on April 30,2025 at 01:20:51 UTC from IEEE Xplore. Restrictions apply.